Transient kinetic studies and microkinetic modelling of primary olefin formation from dimethyl ether over ZSM-5 catalysts

Toyin Omojola[1,2,*], Dmitry B. Lukyanov[1] and Andre C. van Veen[2,*]

[1] Department of Chemical Engineering. University of Bath. Bath. BA2 7AY. UK

[2] School of Engineering. University of Warwick. Coventry. CV4 7AL. UK

***** Correspondence: o.omojola@bath.ac.uk, andre.vanveen@warwick.ac.uk

Abstract

The formation of primary olefins from dimethyl ether (DME) was studied over ZSM-5 catalysts at 300 °C using a novel step response methodology in a temporal analysis of products (TAP) reactor. For the first time, the TAP reactor framework was used to conduct single and multiple step response cycles of DME (balance argon) over a shallow bed with the continuous flow panel. Propylene is the major primary olefin and portrays an S-shaped profile with a preceding induction period when it is not observed in the gas phase. Methanol and water portray overshoot profiles due to their different rates of generation and consumption. DME effluent shows a rapid rise half-way to its steady state value leading to a slow rise thereafter because of its high desorption rates followed by subsequent reactions involving DME in further steps during the induction period. To analyse the experimental data quantitatively, nine reaction schemes were compared and kinetic parameters were obtained by solving a transient plug flow reactor model with coupled dispersion, convection, adsorption, desorption, and reaction steps. The methoxymethyl pathway involving dimethoxyethane and methyl propenyl ether gives the closest match to experimental data in agreement with recent DFT studies. Gaseous dispersion coefficients of *ca.* 10^{-9} m^2 s^{-1} were obtained in the TAP reactor. The novel experimental data validated against the transient kinetic model suggest that after the formation of initial species, the bottleneck in propylene formation is the transformation of the initial C-C bond i.e. dimethoxyethane formed initially from DME and methoxymethyl groups. DME adsorption on ZSM-5 catalyst generates surface methoxy groups which further react with the feed to give methoxymethyl groups. These methoxymethyl groups are regenerated through a series of reactions involving intermediates such as dimethoxymethane and methyl propenyl ether before propylene formation.

Keywords: induction period; hydrocarbon pool; dimethyl ether (DME); temporal analysis of products (TAP) reactor; ZSM-5 zeolite; transient kinetics; MTO; microkinetic model; step response; methanol

1. Introduction

An increasing demand in added-value chemicals and their security as well as incentives to reduce the carbon footprint needed for their generation and utilisation make the conversion of methanol to hydrocarbons (MTH) a viable chemical process. Non-conventional feedstock (such as biomass or organic process waste) and highly abundant resources (such as coal) are used to produce methanol *via* gasification and syngas liquefaction, and can later be transformed to fuels and chemicals over zeolite catalysts (1).

The production of hydrocarbons from methanol under steady-state conditions is regulated by a well-established “hydrocarbon pool” mechanism also known as the dual-cycle consisting of an olefin and aromatic cycle over ZSM-5 catalysts (2-6). The propagation of both cycles over the ZSM-5 catalyst is tunable depending on process conditions (7). Methanol conversion can be tuned towards light olefin production (MTO) at relatively high temperatures and low pressures (8-10).

Methanol undergoes a rapid equilibration process over ZSM-5 catalysts leading to the formation of dimethyl ether (DME) and water (11). There exists a long-standing debate on the evolution of the key oxygenate i.e. methanol and/or DME into the steady-state hydrocarbon pool. The debate centres on: (a) the role of methanol and/or DME, (b) the primary olefin(s) formed and (c) the exact mechanism leading from the key oxygenate to the primary olefin(s).

Various direct mechanisms have been proposed for the conversion of methanol/DME to primary olefins (12). These direct mechanisms are known by their intermediates and include oxonium ylide (13, 14), carbene (15), methane-formaldehyde (16, 17), carbon monoxide (18-20), methoxymethyl (21, 22) and surface methoxy groups (23-26). Using density functional theory (DFT) calculations, Lesthaeghe et al. (27-29) refuted some direct mechanisms based on high activation energy barriers and highly unstable intermediates. Conversely, primary olefins were proposed to form indirectly from impurities (acetone, ethanol) in the methanol feed (30, 31). Hunger and co-workers (23, 24, 32) later observed that the quantity of impurities proposed is insufficient for olefin formation.

Recently, there has been a surge in the evidence for the direct mechanisms leading to primary olefin formation (18, 19, 21, 22). Li et al. (22) gave evidence, using DFT calculations for the formation of propylene from methanol through methoxymethyl cations. In this pathway, 1,2-dimethoxyethane or 2-methoxyethanol were proposed as key intermediates propagating the direct formation of propylene. Wei et al. (21) compared formation pathways involving methane-formaldehyde and methoxymethyl cations for initial C-C bond formation from methanol. They obtained that the most favourable methane-formaldehyde pathway involved the formation of 1,2-ethanediol as the primary C-C bond. Nonetheless, the methoxymethyl pathway was more kinetically and thermodynamically favourable. Liu et al. (18), Chowdhury

et al. (19, 20) and Plessow and Studt (33, 34) provided spectroscopic and theoretical evidence for a carbon monoxide mechanism. The formation of the first C-C bond (surface acetate group) was shown to involve a low activation barrier of 80 kJ mol^{-1}.

Although theoretical calculations have shown the feasibility of the direct pathway involving methoxymethyl cations for the direct formation of ethylene and propylene from methanol, there are no kinetic studies to experimentally validate these proposals. Moreover, there is no kinetic model developed on a microscale level to describe and predict the formation of primary olefins from oxygenates particularly in the induction period.

Recently, we observed that higher temperatures are required to desorb DME in comparison to methanol providing evidence that DME stays longer on the catalysts (35) and is the key oxygenate. This was also evidenced by Liu et al. (18) and Wei et al. (21). In this paper, we investigate the induction period during the formation of primary olefins from DME at 300 °C by conducting novel step response experiments in a temporal analysis of products (TAP) reactor. Nine reaction schemes obtained from literature (18-22) were compared and used as a basis for a microkinetic model. The experimental data was simulated to extract kinetic parameters that describe the formation of primary olefins from DME over fresh ZSM-5 catalysts.

2. Materials and methods

2.1. Experimental

The ammonium form of the fresh ZSM-5 catalyst with a Si/Al ratio of 25, purchased from Zeolyst International, has a crystallite size of 0.10 ± 0.02 µm and an average particle size of 30 µm (35). The ZSM-5 catalysts were pressed, crushed, and sieved to obtain pellet sizes in the range of 250 – 500 µm. Anhydrous DME (99.999%) and argon (99.999%) were purchased from CK special gases Ltd. Experiments were conducted in a transient reactor suited for the temporal analysis of products under close to vacuum conditions. The TAP has three chambers in series: (a) the reactor chamber, (b) the differential chamber and (c) detector chamber. The reactor chamber contains a fixed-bed reactor, 6 mm O.D. (4 mm I.D.) and 40 mm long and has a cone-shaped inset for uniform radial distribution. The differential chamber acts as a cryogenic trap to eliminate scattered molecules reaching the detector chamber where the quadrupole mass spectrometer (QMS) is housed. The differential chamber works as a molecular beam. Gases were introduced through two continuous feeding valves into the reactor inlet. The pressure at the exit of the reactor chamber is maintained at 10^{-5} Pa while the pressure at the end of the differential chamber is 10^{-6} Pa and QMS is 10^{-7} Pa. The response of the QMS, placed in the detector chamber, was calibrated by passing continuous streams of

various gases (methanol, DME, ethylene, propylene, etc.) in argon over an inert quartz bed with particle diameters between 355 – 500 µm. The QMS was operated in a multiple ion detection (MID) mode monitoring a maximum of 10 products simultaneously. The low base pressure (10^{-7} Pa) in the detector chamber allows for high detection sensitivity necessary for quantitative analysis. The inert quartz bed used for calibration had the same length as the catalyst bed. The time required to reach steady state or to drop from steady state was fastest over the inert quartz bed.

10 mg of NH_4-ZSM-5 catalyst was initially decomposed in the TAP reactor chamber by heating it at 10 °C min^{-1} up to 450 °C, holding for 30 min before bringing the sample to 300 °C. Background signal intensities were obtained. The catalyst was then subjected to a steady flow of argon at 10^{-8} mol s^{-1}. Afterwards, the flow was instantaneously switched to a feed of 5 vol% DME in argon (step-up) at a flow rate of *ca*. 4.40×10^{-8} mol s^{-1}. At steady state, the inlet DME feed was instantaneously switched to a steady flow of argon (stopped-flow). Thus, a single step response cycle consists of three phases: step-up, steady-flow and stopped-flow. During the step response cycle, the effluent was monitored with the QMS. Single and multiple step response cycles were carried out.

Flow rates of the inert feed were similar to step response feed and were about 10^{-8} mol s^{-1}, with an inlet pressure of less than 1000 Pa (36). The active catalyst bed length was short (2 mm) compared to the overall bed length of 25 mm (consisting of quartz wool/quartz beads/active catalyst bed/quartz beads/quartz wool).

A novel methodology was developed as described above where ZSM-5 catalysts packed in a shallow bed were subjected to step response of probe molecules under continuous flow. Here, the rate is proportional to the difference of inlet and outlet concentrations. As conversions increase when the TAP reactor is operated as a convective flow device, the level of non-uniformity increases. The extent of the non-uniformity is circumvented in our experiments due to the use of a shallow bed. The above methodology is different from the conventional diffusional flow TAP reactor where the rate is proportional to the difference of inlet and outlet gradient of concentrations (37). Our novel methodology was developed in the TAP reactor to alleviate intricacies associated with the MTH reaction. Olsbye et al. (38) highlighted, in their review, the complexities associated with separating active species and deactivating species during MTO reaction during atmospheric studies. Herein, we show that on multiple step response cycles, deactivation is negligible under TAP conditions. As the pressures used were lower than 1000 Pa, external mass transfer to the particle is negligible due to low gas densities which allow for the absence of a stagnant film around the particle in the TAP reactor. They are suppressed due to negligible intramolecular collisions under vacuum conditions (39). In a previous contribution (35), we also showed that the rates of methanol and DME adsorption and desorption are limiting compared to intra-particle mass

transport contributions. Below (section 4), we show that these rates compete with the rate of transformation of intermediates during the conversion of DME to primary olefins.

Throughout all step response experiments, the temperature and the pressure were constant. The raw data (QMS ion currents) were corrected for background levels and fragmentation contributions for the different molecules and sensitivity factors according to section S1 of supplementary information.

2.2. Modelling

To obtain estimates of the kinetic parameters, the reactor performance was simulated. The outlet concentrations of methanol, DME, water, ethylene and propylene were estimated using the measured inlet conditions of DME and argon in a step function as boundary conditions. Rate parameters were estimated by comparing experiment to model. A one-zone plug flow reactor model was applied. Ideal plug flow was assumed initially due to high gas velocities of the feed expanding to vacuum in the reactor.

Gas:

$$\varepsilon_b \frac{\partial C_{i,g}}{\partial t} = -u \frac{\partial C_{i,g}}{\partial z} - \Gamma_t S_v (1 - \varepsilon_b) R_{i,g} \qquad (2.1)$$

where $R_{i,g}$ is the rate of transformation of species in the gaseous phase and is a function of the concentration ($C_{i,g}$) of specie i in the gaseous phase, mol m^{-3}; ε_b is bed porosity; u is the superficial velocity, m s^{-1}; z is the bed length, m; t is time, s; Γ_t is the concentration of active sites per unit surface area of catalyst (mol m_{cat}^{-2}) and S_v is the catalyst surface area per unit volume (m_{cat}^{-1}). Model properties are given in table 1.

Surface:

$$\frac{\partial \theta_i}{\partial t} = R_{i,s} \qquad (2.2)$$

where $R_{i,s}$ is the rate of transformation of adsorbed species and a function of the surface coverage ($\theta_{i,s}$) of specie i.

Initial condition: t = 0, $C_{i,g} = 0$, $\theta_i = 0$.

Boundary condition: (at t>0, z=0), C_j (0, t) = f(t), j = DME, Ar

The reactor model was solved in MATLAB (version R2016b) using the upwind scheme for solving the hyperbolic 1st order partial differential equation. Backward differencing was applied to the convection term in the PDE. To ensure numerical stability, the Courant-Friedrichs-Lewy (CFL) condition (40) was satisfied:

$$CFL = \left| a \frac{\Delta t}{\Delta z} \right| \leq 1 \qquad (2.3)$$

where $a = u/\varepsilon_b$.

Thereafter, the influence of dispersion was simulated by solving a modification of equation 2.1 for a non-ideal PFR:

$$\varepsilon_b \frac{\partial C_{i,g}}{\partial t} = D_{i,e} \frac{\partial^2 C_{i,g}}{\partial z^2} - u \frac{\partial C_{i,g}}{\partial z} - \Gamma_t S_v (1 - \varepsilon_b) R_{i,g} \quad (2.4)$$

where $D_{i,e}$ is the dispersion coefficient. The broader term dispersion coefficient is used although diffusion may be the main contributor here. Such differentiation cannot be extracted from our experimental data.

The Danckwerts boundary conditions (41) were applied to solving equation 2.4 for DME and argon:

$$C_{i,0} = C_i(0^+) - \frac{D_i}{u} \frac{dC_i(0^+)}{dz} \quad (2.5)$$

$$\frac{dC_i(1^-)}{dz} = 0 \quad (2.6)$$

The sum of square error (SSE) between experiment and model was obtained according to (42, 43):

$$SSE = \sum_{n=1}^{N_c} \sum_{m=1}^{N_d} w_{n,m} \left(Y_{n,m}^{obs} - Y_{n,m}^{cal}\right)^2 \rightarrow min \quad (2.7)$$

where:

n	component number;
m	observation number;
N_c	total number of components;
N_d	total number of observations;
$w_{n,m}$	weighting factor of the m-th observation of component n.
Y^{obs}	experimental data
Y^{cal}	model data

Table 1: Catalyst and reactor properties used in the kinetic model

Parameter	**Value**	**Unit**
Active bed length	2	mm
Overall bed length	25	mm
Si/Al ratio	25	-
Brønsted acid site density	356	µmol g^{-1}
BET surface area	413	m^2 g^{-1}
Γ_t	0.862	µmol m_{cat}^{-2}
ε_b	0.5	-
S_v	2.0×10^5	m_{cat}^{-1}
Velocity, u	0.25	mm s^{-1}

* Brønsted acid site density and BET surface area are obtained from a previous communication (35)

Furthermore, to assess the sensitivity coefficients, the initial rate constants of each elementary step was multiplied by perturbation factors while other rate constants were kept constant. The relative changes in the sum of square error between the experimental and model were obtained with or without the perturbation factor. Subsequently, the sensitivity coefficient was obtained according to:

$$K_s = \frac{\ln(Y_p/Y_o)}{\ln(F)} \tag{2.8}$$

where Y_p and Y_o are the SSE values with or without the perturbation factor and F is the perturbation factor.

The initial parameter estimates were improved greatly by reducing the sum of squares error between model and experiment. Parameter optimisation through the minimisation of the sum of square error using an “fminsearch” function was implemented in MATLAB. The “fminsearch” function uses a Nelder-Mead simplex algorithm as described by Lagarias et al. (44). Nine reaction schemes involving methoxymethyl groups, methane-formaldehyde and carbon monoxide intermediates were compared.

3. Results

Firstly, it was important to establish the full range of gaseous species obtained at steady-state. As shown in Fig. 1, no substantial gaseous products greater than an m/z ratio of 56 was observed.

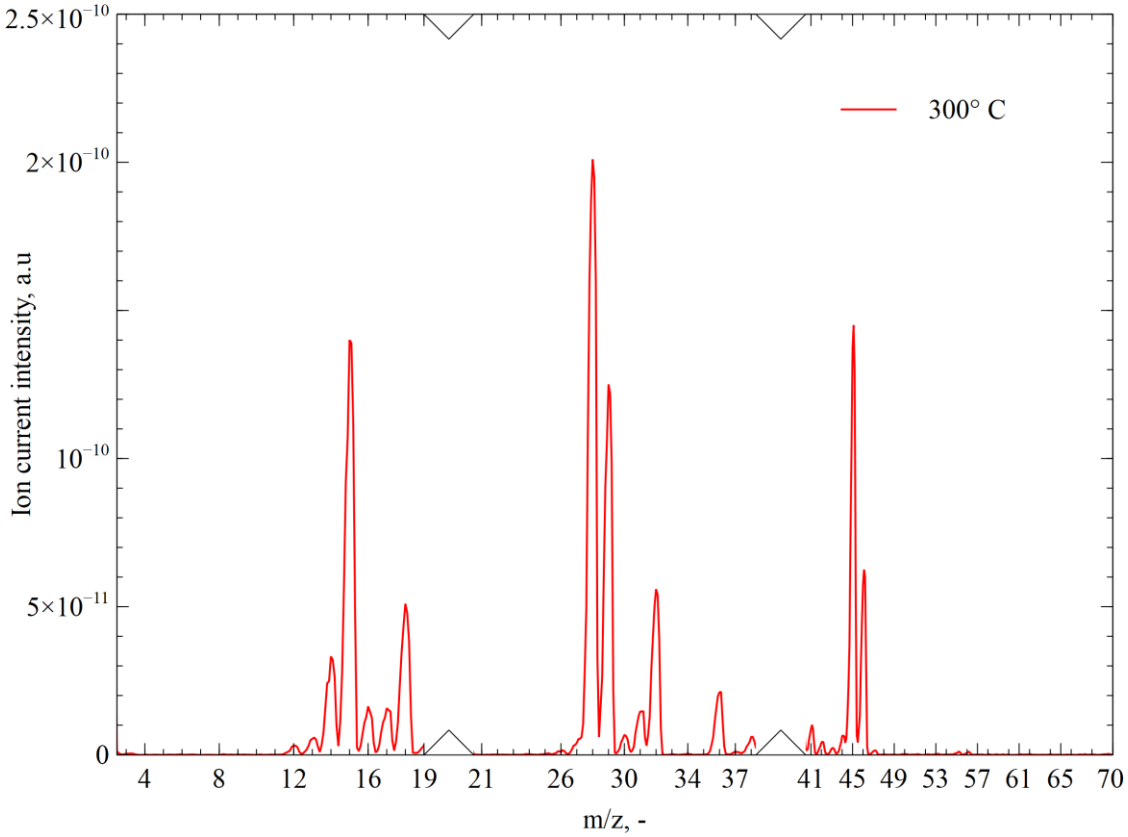

Fig. 1: Full spectrum of gaseous species at steady-state formed after a step response of 5 vol% DME (balance argon) over ZSM-5 (25) catalysts at 300 °C. Argon signals at m/z=20 and 40 have been removed for better clarity.

Propylene (m/z= 41) is the major olefin produced at 300 °C over ZSM-5 catalysts (Figs 1 & 2). The formation of propylene follows an S-shaped profile with a 44-min induction period. The S-shaped propylene profile is caused mainly by the formation of a series of stable intermediates (45, 46) during the induction period leading to the hydrocarbon pool chemistry at steady-state.

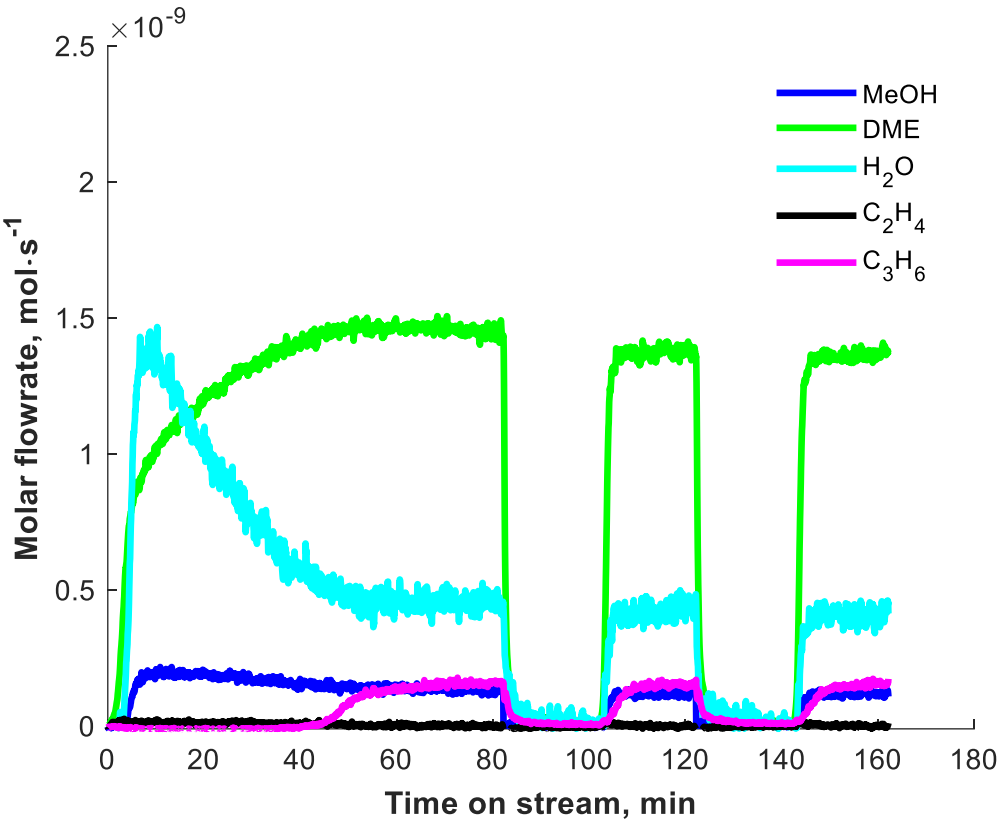

Fig. 2: Step response of 5 vol% DME at 300 °C over 10 mg of ZSM-5 (25) catalysts. Total molar flow rate (5 vol% DME, balance Ar) at STP = 4.4×10^{-8} mol s^{-1}. Steady state conversion is 34.8%

During the induction period of propylene formation, water is generated and released into the gas phase and consumed until steady-state effluent values are reached resulting in a stark overshoot profile. Methanol effluent mirrors this overshoot behaviour although its features are much subtler. DME effluent rises in two stages: rapidly at the beginning and then slowly until it reaches steady state. All effluent species attain steady-state at the same time. Steady-state conversion of DME into hydrocarbons is 34.8%.

After steady molar flowrates of all effluent species were achieved at 300 °C, the catalyst was purged by a flow of argon for 20 min (i.e. after 80 min time on stream in Fig. 2). Subsequently, a second step response cycle of 5 vol% DME was passed over the ZSM-5 catalyst at *ca.* 100 min. As shown in Fig. 2, the initial induction time of propylene effluent observed in the first step response cycle was eliminated. The steady flow of propylene effluent, which follows an S-shaped profile, shows that no deactivation of the catalyst had occurred over the timescale of this experiment at 300 °C. Also, there is no overshoot in the water effluent on subsequent step response cycles. The DME effluent rises immediately in the second and subsequent cycles in comparison to its slower pace in the first cycle.

Nine reaction schemes were compared to explain the induction period observed. These nine reaction schemes are based on the methane-formaldehyde, methoxymethyl and carbon

monoxide pathways. Three routes were analysed for the methane-formaldehyde pathway leading to ethanol (P1), 1,2-ethanediol (P2) and 2-methoxyethanol (P3) as the initial C-C bond (21). Two further routes were analysed that involved the formation of carbon monoxide without Brønsted acid sites (P4) according to the work of Liu et al. (18) or with Brønsted acid sites (P5) according to the work of Plessow and Studt (33) and Anderson and Klinowski (47). Three conventional routes resulting in the formation of the initial C-C bond from the reaction of methoxymethyl groups with methane, methanol and DME leading to ethyl methyl ether (P6), 2-methoxyethanol (P7) and dimethoxyethane (P8) respectively were analysed. A further route was analysed according to the work of Hoang et al. (48) that involves the conversion of dimethoxyethane to methyl propenyl ether which subsequently breaks down to propanal. Propanal forms dimers and trimers and leads to trimethylbenzene, thus initiating the aromatic cycle before ethylene and propylene formation *via* the aromatic dealkylation chemistry (P9). All reaction mechanisms are given in section S2 of the supplementary information. Finally, the effect of dispersion on the P8 route was analysed.

The experimental data was modelled initially using an ideal plug flow reactor model with the various reaction schemes described (table 2). Initial estimates were obtained by comparing experimental data to each model. Parameter optimization was then carried out alongside sensitivity analysis as described in section 2.2 above. The influence of dispersion was then modelled, although the relative proportions between kinetic parameters stayed constant as observed without dispersion.

Table 2: Comparison of different pathways for primary olefin formation from dimethyl ether

Code	Pathway	Initial C-C bond	SSE ($\times 10^{-11}$)
P1	Methane-formaldehyde	Ethanol	2.76
P2		1,2-ethanediol	2.74
P3		2-methoxyethanol	3.21
P4	Carbon monoxide	Surface acetate$^{\wedge}$	7.00
P5		Surface acetate^{+}	11.9
P6	Methoxymethyl	Ethyl methyl ether	2.41
P7		2-methoxyethanol	2.34
P8		Dimethoxyethane$^{\&}$	2.27
P9		Dimethoxyethane$^{\#}$	5.83

^ - carbon monoxide forms in the gas phase
+ - carbon monoxide forms in the presence of Brønsted acid sites
& - pathway involving secondary oxygenates (dimethoxyethane) leading to primary olefins
# - pathway involving secondary oxygenates and an aromatic cycle leading to primary olefins

* Reaction schemes for P1-P7 and P9 are given in section S2 of the supplementary information. Optimised parameters from P2 and P5 are given in section S2 in comparison with P8 given below.

4. Discussion

The debate on the formation of primary olefins is focused on advancing understanding on the mechanism through which the key oxygenate transforms during the induction period. This contribution is focused on the chemical kinetics of DME transformation to primary olefin(s) at low pressures in the TAP reactor at 300 °C. A focus on the chemical kinetics would help elucidate the major bottlenecks involved in primary olefin formation from DME. Ultimately this study fits within the larger framework of quantitatively describing the evolution of the hydrocarbon pool that subsequently regulates product distribution over zeolite and zeotype catalysts at steady-state.

The methane-formaldehyde (16, 17, 29), carbon monoxide (18-20, 33, 34, 47, 49) and methoxymethyl (21, 22) pathways are competing pathways for the direct formation of primary olefins. The first route (P1) following methane and formaldehyde intermediates lead to the formation of ethanol as the initial C-C bond. Ethanol decomposes over ZSM-5 catalysts leading to ethylene as the primary olefin. Ethylene is then methylated by surface methoxy groups to propylene which is observed. This route has been previously suggested to be unfavourable due to the very slow reaction rates for the conversion of methane and formaldehyde to ethanol (29). Yamazaki et al. (50) further showed that the methylation of ethylene to produce propylene occurs at a far slower rate compared to the reaction of DME with surface methoxy groups. Low reaction rates leading to the formation of ethanol as well as negligible rates of the formation of propylene from ethylene and surface methoxy groups lead to the unfavorability of this reaction pathway.

The route leading to the formation of 1,2-ethanediol (P2) is the most favourable methane-formaldehyde pathway following DFT studies (21). The lowest SSE is observed in this route compared to other routes involving methane-formaldehyde intermediates. Double methylation of 1,2-ethanediol leads to the formation of dimethoxyethane which leads to ethylene and propylene formation on decomposition on the ZSM-5 catalysts. A lower agreement is observed for the generation of 2-methoxyethanol (P3) as the initial C-C bond compared to 1,2-ethanediol (P2) from the methane-formaldehyde pathway. This is due to the faster rate of formation of the first C-C bond from the reaction of methanol with adsorbed formaldehyde. The rate of formation of 1,2-ethanediol exceeds 2-methoxyethanol formation by a factor of 5.

Carbon monoxide in pathways P4 and P5 involving surface acetate groups have the effect of reducing the induction time required to form propylene. Carbon monoxide functions as a co-catalyst (33, 34) as the predicted induction time is a factor of 10 times lower than the

observed induction period leading to a high sum of squares error (SSE). The relative mismatch could be due to its negligible contribution at low pressures.

Methoxymethyl pathways are the most thermodynamically and kinetically favourable (21) and as a result have the better agreement amongst the three pathways to experimental data. The route involving dimethoxyethane (P8) shows the best agreement to experimental data given its low SSE and relatively high induction time prediction (Fig. 3). The reaction scheme is given below as:

$$CH_3OCH_3 + HZ \rightleftharpoons CH_3 \cdot Z + CH_3OH \quad (P8.1)$$

$$CH_3OH + HZ \rightleftharpoons CH_3 \cdot Z + H_2O \quad (P8.2)$$

$$H_2O + HZ \rightleftharpoons H_2O \cdot HZ \quad (P8.3)$$

$$CH_3 \cdot Z + CH_3OH \rightleftharpoons CH_3OCH_3 \cdot HZ \quad (P8.4)$$

$$CH_3 \cdot Z + CH_3OCH_3 \rightarrow CH_3OCH_2 \cdot Z + CH_4 \quad (P8.5)$$

$$CH_3OCH_2 \cdot Z + CH_3OCH_3 \rightarrow CH_3OCH_2CH_2OCH_3 \cdot HZ \quad (P8.6)$$

$$CH_3OCH_2CH_2OCH_3 \cdot HZ \rightarrow CH_3CHCHOCH_3 \cdot HZ + H_2O \quad (P8.7)$$

$$CH_3CHCHOCH_3 + HZ \rightleftharpoons CH_3CHCHOCH_3 \cdot HZ \quad (P8.8)$$

$$CH_3CHCHOCH_3 + CH_3 \cdot Z \rightarrow C_3H_6 + CH_3OCH_2 \cdot Z \quad (P8.9)$$

In this scheme, steps P8.if and P8.ib refer to the forward and backward reaction of P8.i respectively. A comparison of experimental data and simulations using initial estimated parameters is given in Fig. S3_P8 (see section S3 of the supplementary information).

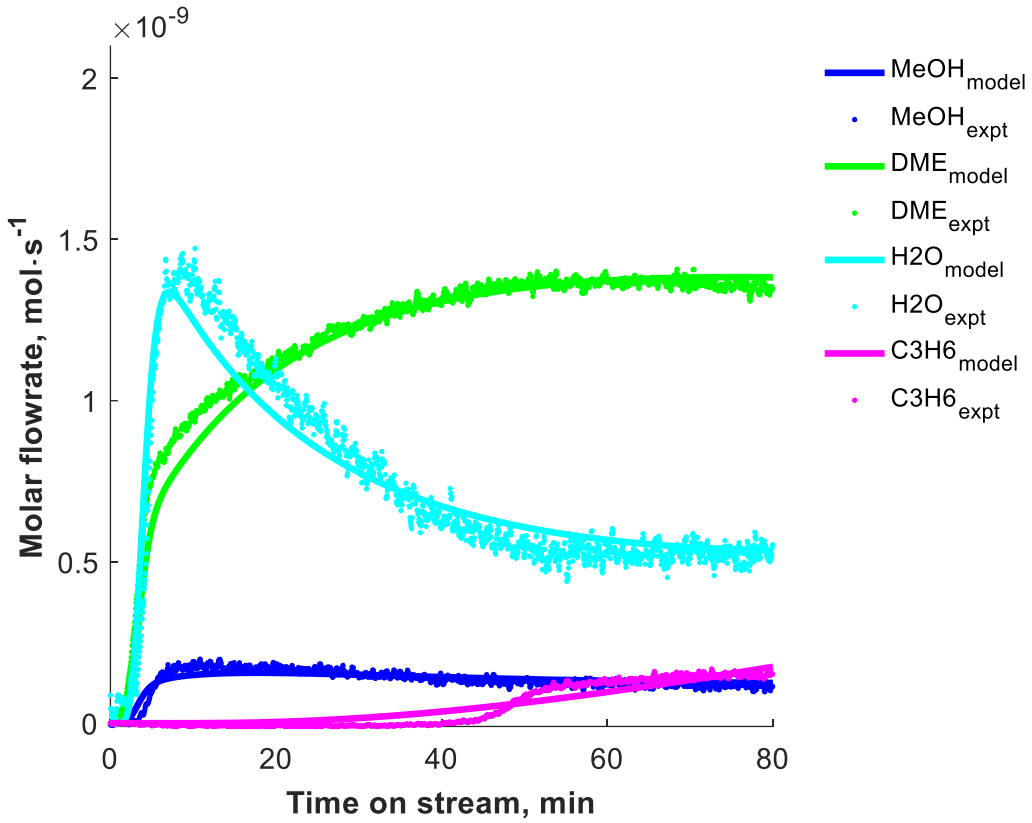

Fig. 3: Step response of DME over ZSM-5 catalysts at 300 °C using optimised parameters

The dissociative adsorption, and desorption of DME, methanol and water as well as the reaction of surface methoxy groups and methanol govern their initial release into the gas phase and the early concentrations of methoxy groups on the catalyst surface. The desorption of DME is much faster than its adsorption and the desorption of methanol is faster than its adsorption. DME desorption is faster than methanol desorption under reactive conditions (table 3). Gaseous DME reacts with surface methoxy groups and methoxy methyl groups in reaction steps P8.5 and P8.6 to produce methoxymethyl groups and dimethoxyethane respectively. The higher reverse dissociation rate of gaseous DME (step P8.1) on the active site is necessary to supply its gaseous form needed for reactions later (steps P8.5 and P8.6) during the induction period. In Fig. 3, DME effluent reaches steady state slowly following an initial rapid rise. The initial rapid rise is due to a fast-backward rate constant in step P8.1 leading to large releases of DME into the gas phase. The slower rate of rise following afterwards is due to the reactions involving DME in steps P8.5 and P8.6 later during the induction period. Alternatively, it could be due to DME saturation on the active sites ZSM-5 catalyst if molecular adsorption is considered. A better fit has been obtained with dissociative adsorption, however.

Table 3: Parameters for the conversion of DME to propylene over ZSM-5 catalysts in a TAP reactor*

Parameters	Initial estimates (ideal PFR)	Optimised values (ideal PFR)	Values (non-ideal PFR)	Unit
k_{1f}	0.00045	0.000421		$Pa^{-1}\ s^{-1}$
k_{1b}	5.2	4.27		$Pa^{-1}\ s^{-1}$
k_{2f}	0.00182	0.00253		$Pa^{-1}\ s^{-1}$
k_{2b}	0.1010	0.468		$Pa^{-1}\ s^{-1}$
k_{3f}	0.0003	0.000142		$Pa^{-1}\ s^{-1}$
k_{3b}	50	152		s^{-1}
k_{4f}	0.00028	7.85e-8		$Pa^{-1}\ s^{-1}$
k_{4b}	1.7	0.215		s^{-1}
k_{5f}	0.02	0.028		$Pa^{-1}\ s^{-1}$
k_{6f}	0.5	0.469		$Pa^{-1}\ s^{-1}$
k_{7f}	0.129	0.0973		s^{-1}
k_{8f}	0.00375	0.00878		$Pa^{-1}\ s^{-1}$
k_{8b}	812.5	1.24		s^{-1}
k_{9f}	125	10.5		$Pa^{-1}\ s^{-1}$

*kif and kib refer to forward and backward rate constant of reaction step P8.i.

Surface methoxy groups are generated early in the induction period and consumed later leading to the formation of intermediates and propylene. Slow generation of surface methoxy groups occurs given the dissociation rates of DME and methanol in reaction steps P8.1f and P8.2f respectively. Surface methoxy groups are also slowly consumed leading to the formation of adsorbed DME (step P8.4f) and generation of methoxymethyl groups (step P8.5f). However, they are rapidly consumed in step P8.9f leading to the formation of propylene.

Water effluent portrays an overshoot profile with time on stream. The water effluent is controlled by its molecular adsorption and desorption (step P8.3) and the dissociative adsorption and desorption of methanol (step P8.2) and the formation of methyl propenyl ether from dimethoxyethane (step P8.7). Methanol adsorption and desorption leads to little concentrations of water in the gas phase (step P8.2). Once formed, water remains mostly in the gas phase (step P8.3). Step P8.7f shows a large reaction rate constant for water formation from dimethoxyethane. Although water is rapidly produced in step P8.7f and rapidly desorbed in step P8.3b, it reacts rapidly with surface methoxy groups to give methanol in step P8.2b. Thus, the overshoot in water effluent is due to the competing dynamics governing its formation and consumption during the induction period.

Gaseous methanol effluent is affected by the early reactions (steps P8.1, P8.2 and P8.4). Desorption rates greater than adsorption rates in steps P8.1 and P8.2 lead to a slow release of methanol in the gas phase. In step P8.4f, methanol is slowly consumed, although the rate of reaction is slower than its nominal formation rate in steps P8.1f and P8.2b. Thus, small concentrations of methanol are generated in steps P8.1 and P8.2, which are slowly consumed in step P8.4 during the induction period. The difference between the rates of methanol

formation and consumption is responsible for its slight overshoot depicted in Fig. 3. Methanol overshoot effectively mirrors water overshoot except that its features are subtler. This is probably due to reaction step P8.2. connecting methanol, water and surface methoxy groups.

Propylene is formed very rapidly (step P8.9f) from the initial species (methanol, DME, water, surface methoxy groups, methoxymethyl groups) through a series of intermediates (dimethoxyethane and methyl propenyl ether). Both intermediates are readily available in the pores of the ZSM-5 catalyst and in the gas phase due to high desorption rates respectively. After the formation of initial species (methanol, DME, water, surface methoxy groups and methoxymethyl groups), the bottleneck in propylene formation which is also a very important step according to the sensitivity analysis (Fig. 4) is the transformation of dimethoxyethane (step P8.7) formed initially from DME and methoxymethyl groups (step P8.6).

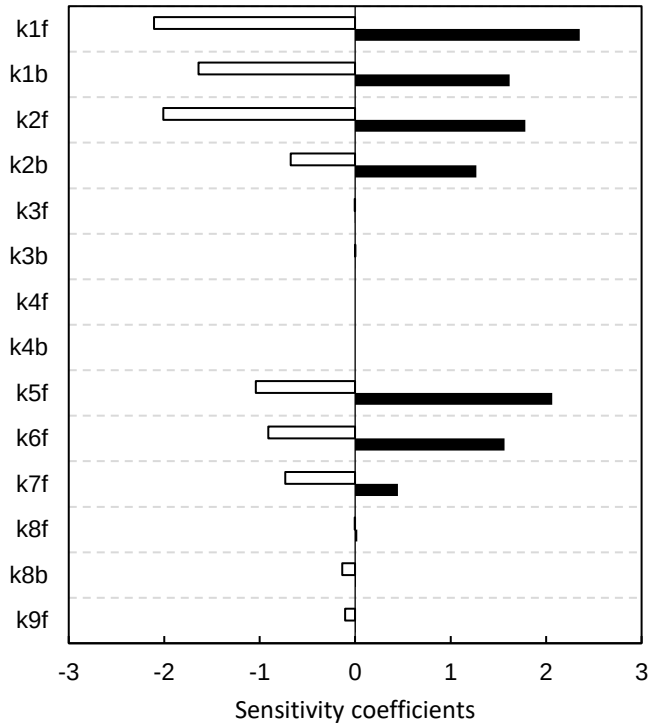

Fig. 4: Sensitivity analysis for elementary steps involved in the formation of propylene from DME over ZSM-5 catalysts at 300 °C

Kobayashi (45, 46) observed that an S-shaped profile observed during the induction period is due to the slow transformation of several stable intermediates. Hoang et al. (48) proposed reaction pathways that looked at the formation of dimers and trimers of aldehydes leading to aromatics formation which consequently dealkylate to give primary olefins. We modelled this pathway (P9) allowing for the formation of secondary oxygenates and aromatics before primary olefin formation. We observed that to obtain the detected propylene selectivity, the transformation rates between secondary oxygenates and aromatics must be rapid. The

high rates of transformation, however lead to lower induction times. The induction times are accurately predicted only at low rates of dimer and trimer transformation but leading to lower propylene selectivities than those observed. Based on the pathway giving the lowest sum of squares error, the dimethoxymethane route of the methoxymethyl pathway, as suggested by Fan and co-workers (21, 22) gives the closest agreement to experimental data.

The inclusion of the steady-state hydrocarbon pool chemistry along with the induction period chemistry (as investigated in this paper) would lead to a full description of the S-shaped propylene profile observed. It is beyond the scope here to investigate the effect of the hydrocarbon pool chemistry on the S-shaped propylene profile and indeed there are already collections of review articles (7, 12) on this topic. As soon as the primary olefin is formed in the induction period, olefin methylation, oligomerisation and cracking, and hydrogen transfer and cyclisation as well as aromatic methylation and dealkylation chemistries regulate steady-state conversion of initial oxygenates (methanol, DME) to hydrocarbons. Nonetheless, in this article, we have provided mechanistic insights on the challenges of the chemistries occurring only during the induction period.

Yablonsky et al. (51) proposed a reactive mixing index analysis (REMI) function for diagnostics of the hydrodynamic regime during ideal and non-ideal flow of pulse inputs into the TAP reactor. The REMI criterion for the characterization of the mixing quality in a catalytic reactor which, initially at steady-state, is perturbed by small pulses of a chemical reactant. CSTR, ideal PFR and non-ideal PFR were considered. In our analysis, step response has been carried out using the continuous feeding valves of the TAP reactor over a shallow bed hence representing the non-ideal PFR as convection and dispersion effects were considered. The effects of dispersion were modelled using equation 2.4 and dispersion coefficients were of the order of *ca.* 10^{-9} m^2 s^{-1}. The trend observed in rate constants without dispersion effects were the same as those when dispersion was included in the model.

5. Conclusions

The formation of primary olefins from dimethyl ether (DME) has been studied over ZSM-5 catalyst using a novel step response methodology in a temporal analysis of products (TAP) reactor. Propylene is the major olefin formed at 300 °C and portrays an S-shaped profile. Overshoot profiles are depicted by methanol and water with time on stream. DME effluent reaches its steady state flowrate in two phases: rapidly up until half its steady-state value and then slowly. The results were explained using a transient kinetic model that considers dispersion, convection, adsorption, desorption and reaction for step response cycles applied to ZSM-5 catalysts in a shallow bed packing configuration. Nine reaction schemes were tested using recent density functional theory studies. The methoxymethyl pathway involving

dimethoxyethane as the first C-C bond gives the closest agreement to experiment. After the formation of primary products (methanol, water, surface methoxy groups, methoxymethyl groups and methane) from DME, the transformation of the first C-C bond (reaction of methoxymethyl group with DME to give dimethoxyethane) represents the major bottleneck in propylene formation over ZSM-5 catalysts.

6. Acknowledgements

Financial support from the Petroleum Technology Development Fund of Nigeria (PTDF/ED/PHD/OO/766/15) and from the European Commission in the scope of the 7th Framework program BIOGO project (grant number: 604296) https://www.biogo.eu/ is acknowledged. T. Omojola is grateful for fruitful discussions with Dr Waleed Ali (Department of Mathematics, University of Bath).

7. Notes

The authors declare no conflict of interest.

8. References

1. Tian P, Wei Y, Ye M, Liu Z. Methanol to olefins (MTO): From fundamentals to commercialization. ACS Catalysis. 2015;5(3):1922-38.
2. Dahl IM, Kolboe S. On the reaction mechanism for propene formation in the MTO reaction over SAPO-34. Catal Lett. 1993;20(3-4):329-36.
3. Dahl IM, Kolboe S. On the Reaction Mechanism for Hydrocarbon Formation from Methanol over SAPO-34. I. Isotopic Labeling Studies of the Co-Reaction of Ethene and Methanol. J Catal. 1994;149(2):458-64.
4. Dahl IM, Kolboe S. On the reaction mechanism for hydrocarbon formation from methanol over SAPO-34: 2. Isotopic labeling studies of the Co-reaction of propene and methanol. J Catal. 1996;161(1):304-9.
5. Olsbye U, Bjørgen M, Svelle S, Lillerud KP, Kolboe S. Mechanistic insight into the methanol-to-hydrocarbons reaction. International Conference on Gas-Fuel 05. 2005;106(1-4):108-11.
6. Bjørgen M, Svelle S, Joensen F, Nerlov J, Kolboe S, Bonino F, et al. Conversion of methanol to hydrocarbons over zeolite H-ZSM-5: On the origin of the olefinic species. J Catal. 2007;249(2):195-207.
7. Ilias S, Bhan A. Mechanism of the catalytic conversion of methanol to hydrocarbons. ACS Catalysis. 2013;3:18-31.
8. Vora BV, Marker TL, Barger PT, Nilsen HR, Kvisle S, Fuglerud T. Economic route for natural gas conversion to ethylene and propylene. In: Pontes Md, Espinoza RL, Nicolaides CP, Scholtz JH, Scurrell MS, editors. Stud Surf Sci Catal. Volume 107: Elsevier; 1997. p. 87-98.
9. Koempel H, Liebner W. Lurgi's Methanol To Propylene (MTP®) Report on a successful commercialisation. Stud Surf Sci Catal2007. p. 261-7.
10. Chang CD, Lang WH, Smith RL. The conversion of methanol and other O-compounds to hydrocarbons over zeolite catalysts. II. Pressure effects. J Catal. 1979;56(2):169-73.

11. Svelle S, Kolboe S, Swang O, Olsbye U. Methylation of Alkenes and Methylbenzenes by Dimethyl Ether or Methanol on Acidic Zeolites. The Journal of Physical Chemistry B. 2005;109(26):12874-8.
12. Stöcker M. Methanol-to-hydrocarbons: Catalytic materials and their behavior. Microporous Mesoporous Mater. 1999;29(1-2):3-48.
13. Mole T, Whiteside JA. Conversion of methanol to ethylene over ZSM-5 zeolite in the presence of deuterated water. J Catal. 1982;75(2):284-90.
14. Mole T. Conversion of methanol to ethylene over ZSM-5 zeolite: A reexamination of the oxonium-ylide hypothesis, using 13carbon- and deuterium-labeled feeds. J Catal. 1983;84(2):423-34.
15. Dass DV, Martin RW, Odell AL, Quinn GW. A Re-Examination of Evidence for Carbene (CH2:) As An Intermediate in the Conversion of Methanol to Gasoline. The Effect of Added Propane. In: Bibby DM, Chang CD, Howe RF, Yurchak S, editors. Stud Surf Sci Catal. 36: Elsevier; 1988. p. 177-81.
16. Nováková J, Kubelková L, Habersberger K, Dolejšek Z. Catalytic activity of dealuminated Y and HZSM-5 zeolites measured by the temperature-programmed desorption of small amounts of preadsorbed methanol and by the low-pressure flow reaction of methanol. Journal of the Chemical Society, Faraday Transactions 1: Physical Chemistry in Condensed Phases. 1984;80(6):1457-65.
17. Dewaele O, Geers VL, Froment GF, Marin GB. The conversion of methanol to olefins: A transient kinetic study. Chem Eng Sci. 1999;54(20):4385-95.
18. Liu Y, Müller S, Berger D, Jelic J, Reuter K, Tonigold M, et al. Formation Mechanism of the First Carbon-Carbon Bond and the First Olefin in the Methanol Conversion into Hydrocarbons. Angewandte Chemie - International Edition. 2016;55(19):5723-6.
19. Chowdhury AD, Houben K, Whiting GT, Mokhtar M, Asiri AM, Al-Thabaiti SA, et al. Initial Carbon–Carbon Bond Formation during the Early Stages of the Methanol-to-Olefin Process Proven by Zeolite-Trapped Acetate and Methyl Acetate. Angewandte Chemie - International Edition. 2016;55(51):15840-5.
20. Chowdhury AD, Paioni AL, Houben K, Whiting GT, Baldus M, Weckhuysen BM. Bridging the Gap between the Direct and Hydrocarbon Pool Mechanisms of the Methanol-to-Hydrocarbons Process. Angewandte Chemie - International Edition. 2018.
21. Wei Z, Chen YY, Li J, Guo W, Wang S, Dong M, et al. Stability and Reactivity of Intermediates of Methanol Related Reactions and C-C Bond Formation over H-ZSM-5 Acidic Catalyst: A Computational Analysis. Journal of Physical Chemistry C. 2016;120(11):6075-87.
22. Li J, Wei Z, Chen Y, Jing B, He Y, Dong M, et al. A route to form initial hydrocarbon pool species in methanol conversion to olefins over zeolites. J Catal. 2014;317(0):277-83.
23. Wang W, Buchholz A, Seiler M, Hunger M. Evidence for an Initiation of the Methanol-to-Olefin Process by Reactive Surface Methoxy Groups on Acidic Zeolite Catalysts. J Am Chem Soc. 2003;125(49):15260-7.
24. Jiang Y, Wang W, Marthala VRR, Huang J, Sulikowski B, Hunger M. Effect of organic impurities on the hydrocarbon formation via the decomposition of surface methoxy groups on acidic zeolite catalysts. J Catal. 2006;238(1):21-7.
25. Jiang Y, Wang W, Reddy Marthala VR, Huang J, Sulikowski B, Hunger M. Response to comments on the paper: "Effect of organic impurities on the hydrocarbon formation via the decomposition of surface methoxy groups on acidic zeolite catalysts" by Y. Jiang, W. Wang, V.R.R. Marthala, J. Huang, B. Sulikowski, M. Hunger. J Catal. 2006;244(1):134-6.
26. Ono Y, Mori T. Mechanism of methanol conversion into hydrocarbons over ZSM-5 zeolite. Journal of the Chemical Society, Faraday Transactions 1: Physical Chemistry in Condensed Phases. 1981;77(9):2209-21.

27. Lesthaeghe D, Van Speybroeck V, Marin GB, Waroquier M. Understanding the failure of direct C-C coupling in the zeolite-catalyzed methanol-to-olefin process. Angewandte Chemie - International Edition. 2006;45(11):1714-9.
28. Lesthaeghe D, Van Speybroeck V, Marin GB, Waroquier M. What role do oxonium ions and oxonium ylides play in the ZSM-5 catalysed methanol-to-olefin process? Chem Phys Lett. 2006;417(4-6):309-15.
29. Lesthaeghe D, Van Speybroeck V, Marin GB, Waroquier M. The rise and fall of direct mechanisms in methanol-to-olefin catalysis: An overview of theoretical contributions. Ind Eng Chem Res. 2007;46(26):8832-8.
30. Goguen PW, Xu T, Barich DH, Skloss TW, Song W, Wang Z, et al. Pulse-quench catalytic reactor studies reveal a carbon-pool mechanism in methanol-to-gasoline chemistry on zeolite HZSM-5. J Am Chem Soc. 1998;120(11):2650-1.
31. Song W, Marcus DM, Fu H, Ehresmann JO, Haw JF. An oft-studied reaction that may never have been: Direct catalytic conversion of methanol or dimethyl ether to hydrocarbons on the solid acids HZSM-5 or HSAPO-34. J Am Chem Soc. 2002;124(15):3844-5.
32. Wang W, Seiler M, Hunger M. Role of surface methoxy species in the conversion of methanol to dimethyl ether on acidic zeolites investigated by in situ stopped-flow MAS NMR spectroscopy. J Phys Chem B. 2001;105(50):12553-8.
33. Plessow PN, Studt F. Unraveling the Mechanism of the Initiation Reaction of the Methanol to Olefins Process Using ab Initio and DFT Calculations. ACS Catalysis. 2017;7(11):7987-94.
34. Plessow PN, Studt F. Theoretical Insights into the Effect of the Framework on the Initiation Mechanism of the MTO Process. Catal Lett. 2018;148(4):1246-53.
35. Omojola T, Cherkasov N, McNab AI, Lukyanov DB, Anderson JA, Rebrov EV, et al. Mechanistic Insights into the Desorption of Methanol and Dimethyl Ether Over ZSM-5 Catalysts. Catal Lett. 2018;148(1):474-88.
36. Hinrischen O, van Veen AC, Zanthoff HW, Muhler M. TAP Reactor Studies. In: Haw JF, editor. In-Situ Spectroscopy in Heterogeneous Catalysis. WeinHeim: Wiley-VCH; 2002.
37. Marin GB, Yablonsky GS. Kinetics of Chemical Reactions: Decoding Complexity Weinheim, Germany: WILEY-VCH; 2011. 1-428 p.
38. Olsbye U, Svelle S, Lillerud KP, Wei ZH, Chen YY, Li JF, et al. The formation and degradation of active species during methanol conversion over protonated zeotype catalysts. Chem Soc Rev. 2015;44(20):7155-76.
39. Van Veen AC, Zanthoff HW, Hinrichsen O, Muhler M. Fixed-bed microreactor for transient kinetic experiments with strongly adsorbing gases under high vacuum conditions. Journal of Vacuum Science and Technology, Part A: Vacuum, Surfaces and Films. 2001;19(2):651-5.
40. Courant R, Friedrichs K, Lewy H. Über die partiellen Differenzengleichungen der mathematischen Physik. Mathematische Annalen. 1928;100(1):32-74.
41. Danckwerts PV. Continuous flow systems: Distribution of residence times. Chem Eng Sci. 1953;2(1):1-13.
42. Van Der Linde SC, Nijhuis TA, Dekker FHM, Kapteijn F, Moulijn JA. Mathematical treatment of transient kinetic data: Combination of parameter estimation with solving the related partial differential equations. Applied Catalysis A: General. 1997;151(1):27-57.
43. Rasmuson A, Andersson B, Olsson L, Andersson R. Mathematical Modeling in Chemical Engineering USA: Cambridge University Press; 2014.
44. Lagarias JC, Reeds JA, Wright MH, Wright PE. Convergence properties of the Nelder-Mead simplex method in low dimensions. SIAM Journal on Optimization. 1998;9(1):112-47.
45. Kobayashi M. Characterization of transient response curves in heterogeneous catalysis—I Classification of the curves. Chem Eng Sci. 1982;37(3):393-401.

46. Kobayashi M. Characterization of transient response curves in heterogeneous catalysis - 2. Estimation of the reaction mechanism in the oxidation of ethylene over a silver catalyst from the mode of the transient response curves. Chem Eng Sci. 1982;37(3):403-9.
47. Anderson MW, Klinowski J. Solid-state NMR studies of the shape-selective catalytic conversion of methanol into gasoline on zeolite ZSM-5. J Am Chem Soc. 1990;112(1):10-6.
48. Hoang TQ, Zhu X, Sooknoi T, Resasco DE, Mallinson RG. A comparison of the reactivities of propanal and propylene on HZSM-5. J Catal. 2010(271).
49. Jackson JE, Bertsch FM, Bertsch FM. Conversion of Methanol to Gasoline: A New Mechanism for Formation of the First Carbon-Carbon Bond. J Am Chem Soc. 1990;112(25):9085-92.
50. Yamazaki H, Shima H, Imai H, Yokoi T, Tatsumi T, Kondo JN. Direct production of propene from methoxy species and dimethyl ether over H-ZSM-5. Journal of Physical Chemistry C. 2012;116(45):24091-7.
51. Yablonsky GS, Constales D, Marin GB. A new approach to diagnostics of ideal and non-ideal flow patterns: I. The concept of reactive-mixing index (REMI) analysis. Chem Eng Sci. 2009;64(23):4875-83.